

Preparation, Characterization and Activity of CoMo supported on graphene for Heavy Naphtha Hydro-desulfurization reaction

Hameed Hussein Alwan^{a*}, Hasan F. Makki^b, and Tahseen A. Al-Hattab^a

a) Chemical Engineering Department, College of Engineering, University of Babylon, Iraq

b) Chemical Engineering Department, College of Engineering, University of Baghdad, Iraq

Received 23 December 2020; received in revised form 16 May 2021; accepted 17 May 2021

ABSTRACT

Cobalt and Molybdenum oxides supported on graphene catalyst CoMo/G were prepared then its activity for hydro-desulfurization reaction HDS was examined in this research. The catalyst was characterized by X-ray diffraction XRD, Fourier transform infrared spectroscopy FTIR, and energy dispersive spectroscopy EDS while surface morphology was tested by scanning electronic microscopy SEM and atomic force microscopy AFM. The texture properties (specific surface area and pore volume) are measured by the Brunauer, Emmett and Teller BET method. The catalyst activity investigation was conducted by heavy naphtha HDS reaction in a fixed bed reactor, this study investigated the effect of temperature (250-325) °C, Liquid Hourly Space Velocity LHSV (3-6) hr⁻¹ and hydrogen partial pressure (1-1.3) MPa while gas/oil ratio was kept a constant 50 ml/ml, these variables' impact was designed and analyzed by Taguchi design of experiment DOE with using MINITAB software. The results showed that sulfur removing percentage SR% increases with both increasing of temperature and hydrogen partial pressure whereas LHSV has the opposite effect on SR%. HDS reaction kinetics parameters were estimated by experiment results employing Levenberg-Marquardt and SPSS software version 20; the results showed the HDS reaction which followed 1.863 order, reaction rate constant and activation energy, is 32.309 kJ/mol.

Keywords: Heavy Naphtha, CoMo catalyst, graphene, hydro-desulfurization, reaction kinetics, Taguchi method, Levenberg-Marquardt algorithm.

1. Introduction

Crude oil contains many potentially dangerous compounds such as sulfur, nitrogen and oxygen organic compounds: which may cause bad consequences especially when using petroleum products as fuel, resulting in the production of nitrogen dioxide (NO₂), sulfur dioxide (SO₂), and carbon oxide (CO) emissions, which cause air pollutants. NO₂ has caused catastrophic injury to humans, including death; ambient NO₂ exposure may increase the risk of respiratory tract infections through the pollutant's interaction with the immune system and Sulfur dioxide (SO₂) contributes to respiratory symptoms in both healthy patients and those with underlying pulmonary disease [1].

Sulfur organic compounds may take many forms such as thiol (RS-H), sulfides (R-S-R), thiophene (C₄H₄S) and thiophene derivatives e.g. benzothiophene (C₈H₆S) and dibenzothiophene (C₁₂H₈S). These components caused bad consequences such as increasing of sulfur oxides emissions that cause acid rain and environmental pollution, as well as causing problems to human and animal health. On the other hand, corrosion occurred for metallic equipment in refineries and high catalyst poisoning at reforming unit were caused by presence of sulfur components [2].

There are many techniques that are used for removing sulfur from fuel e.g. hydro-desulfurization HDS, extraction, oxidation, alkylation, adsorption, bio-desulfurization, membrane separation and their combinations, but the traditionally used HDS process has been proposed to remove sulfur from fuel liquid by using a catalyst under high temperature and pressure in the existence of hydrogen. HDS reaction is very

*Corresponding author.

E-mail address: hameed@uobabylon.edu.iq

(H. H. Alwan)

effective for reducing thiol, sulfide and sulfide, but aromatic sulfur compounds such as thiophene and its derivatives are and less reactive in the HDS process [3]. The classic catalysts for HDS reactions are alumina, silica, or silica - supporting metal oxides such as cobalt, molybdenum, molybdenum nickel, and tungsten nickel. The Co(Ni)Mo(W)/Al₂O₃ catalysts have been applied in petroleum refineries for over half a century [2, 4]. HDS process was performed at higher temperature and pressure in the presence of a suitable catalyst, the process operation conditions were dependent on feed stock used and the required specifications, for example the reaction temperature, hydrogen pressure, LHSV and H₂/oil required for naphtha hydro-treating HDT are 320 °C, 1-2 MPa, 3-8 hr⁻¹ and 60 Nm³/m³ respectively while for vacuum gas oil HDT are 360°C, 5-9 MPa, 1-2 hr⁻¹ and 210 Nm³/m³ respectively [5].

The great challenge of catalytic synthesis is to produce a high activity and selectivity catalyst, and also catalyst support which has the ability for overcoming high interaction between the active metal and the support. Some researchers suggested carbon and its allotropes for using catalyst carrier (support) because carbon is characterized by its high activity, the ease of recovery from catalyst waste, and lower coke formation. Graphene is a monolayer of carbon atoms that contains honey and is one of the most important carbon allotropes because of its high surface area with high mechanical, chemical and thermal stability. There are many examples for using graphene as catalyst support such as Cobalt and molybdenum supported on graphene CoMo/G [6], iron oxide supported on graphene NiMo/G for desulfurization oxidation [7] and Copper and palladium/copper nanoparticles supported on reduced graphene oxide catalysts were synthesized and evaluated for the selective NO reduction by CO [8] etc. In this process, the catalyst activity of CoMo supported on graphene for heavy naphtha desulfurization by HDS reaction was studied. The catalyst was prepared by co-precipitation of Cobalt and molybdenum on a graphene surface. This piece of work examines the sulfur removal under specific operation conditions for HDS reaction, where this study was carried out by using Taguchi method experimental design with four levels for each of three variables (reaction temperature, space velocity and hydrogen partial pressure). By using Minitab software the effect of studied variables was analyzed and the process was optimized, also the HDS reaction kinetics were investigated by applying Levenberg-Marquardt.

2. Experimental

2.1 Materials

Heavy naphtha (with boiling point range 30-175 °C, total sulfur content 755 ppm, specific gravity 0.694) was provided by Al-Najaf refinery, hydrogen gas with 99% purity, sulfuric acid (H₂SO₄) with 99% purity by (CHD Ltd.), nitric acid (HNO₃) with 65% purity by (CHD Ltd.), ammonium heptamolybdate (NH₄)₆Mo₇O₂₄·4H₂O AHM with 99% purity by (HOPKIN & WILLIAMS), cobalt nitrate (Co(NO₃)₂·6H₂O) with 99% purity by (CHD Ltd.), PVA (Mw = 9,000-10,000[-CH₂CHOH-]_n) by (Sigma). The graphene was synthesized by dehydration of Iraqi date syrup [9].

2.2 Catalyst Preparation

The graphene synthesized by dehydration of Iraqi date syrup surface was functionalized with sulfuric acid (99%) and nitric acid (65%) mixture (3:1) by volume under sonication (MTI corporation, SJIA-1200 W) at 500 watt for 1 hour to form functional groups on graphene sheets, this technique is oxidation nanostructure which introduces carboxylic group (-COOH) or any other oxygen group such as carbonyl (-C=O), and ester (-COOR) group. The developed functionalized groups were formed at defects sites on the graphene surface which assist loading required metal oxides. Functionalized graphene was filtered and finally dried at 110 °C under vacuum for two hours. For impregnation 10 g from functionalized graphene, prepare two solutions were prepared; in the first solution, 1.857 g of AHM ((NH₄)₆Mo₇O₂₄·4H₂O) salt (as molybdenum oxide source) and in the second solution, 2.3513 g of cobalt nitrate hexahydrate (Co(NO₃)₂·6H₂O) salt (as nickel oxide source) dissolved in distilled water. These two solutions were added, followed loaded on Graphene surface by co-impregnation method to precipitate cobalt and molybdenum oxides about 6 wt.% and 15% respectively. The impregnated Graphene was dried at 110 °C for two hours and calcination was done at 400°C for two hours [6]. Finally, prepared catalyst CoMo/G was formulated with 5 wt. % Polyvinyl alcohol PVA (as a binder), and the final shape for preparing catalysts was an extrudate as shown in **Fig. 1**. MoO₃ converted to MoS₂ by sulfiding step, in which gas oil was used as the sulfiding agent [10].

2.3 Catalyst Characterizations

The prepared catalyst was characterized by X-ray diffraction (XRD) Shimadzu Model XRD- 6000, Fourier-Transform infrared spectroscopy (FTIR), BRUKER Model PLATINUM-ATR Alpha series and Energy-dispersive X-ray spectroscopy (DES) BRUKER



Fig. 1. Extruded final product (CoMo/G catalyst)

Model X Flash 6110 Germany). The morphology test of the catalyst was done by Scanning electronic microscopy (SEM) FEI model QUANTA 450 and Atomic force microscopy (AFM) Angstrom, Model AA3000 Advanced Inc., AA3000; while surface area and pore volume were estimated by the BET method by using Thermo Analyzer/USA.

2.4 Catalyst activity

CoMo/G catalyst activity was investigated by heavy naphtha HDS reaction by using hydro-desulfurization unit as shown in **Fig. 2**, the HDS unit contains a fixed bed reactor (20 mm in diameter and 600 mm length), the fixed bed reactor was divided into three zones; top zone and bottom zone were filled with inert bed and the middle zone contained 57 grams of catalyst (CoMo/G). The sulfur removal was examined under impact of reaction temperature, LHSV and hydrogen pressure by use of Taguchi experiment design. The initial and final sulfur contents were measured by using sulfur meter (RX-620SA/TANKA SCITIFIC), sulfur removal efficiency SR% was calculated according to **equation (1)**:

$$SR\% = \frac{S_0 - S_f}{S_0} \times 100 \quad (1)$$

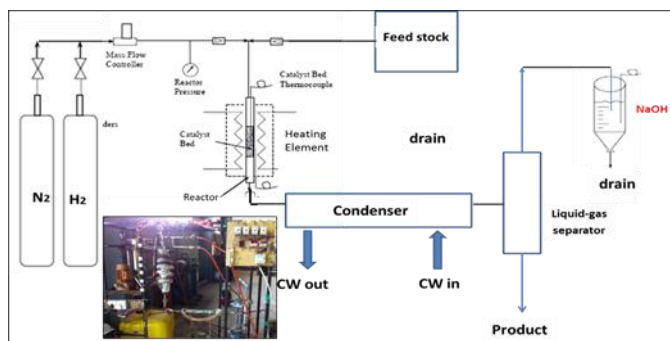


Fig. 2. hydro-desulfurization unit flow sheet the inset figure is the hydro-desulfurization unit.

Where $S\%$, S_f and S_o are sulfur removal efficiency, sulfur content in product and sulfur content in feed respectively.

3. Result and Discussion

3.1. Catalyst characterization

XRD is an important tool used for design and production catalysts because it can offer good information on bulk structure and solid composition as well as analyzing unit cell size and its crystallite, in which the crystallite size can be determined by XRD by peak width analysis. Fig.3 shows XRD pattern for the prepared catalyst, as shown, there are several diffraction angles at about $2\theta = 23.3, 47.3, 53.5$ and 54.5° which may have referred to the formation of CoMoO_4 phase with good agreement with JCPDS card#86-0361 [9], while 37.5° peak corresponds to the presence of Co_3O_4 as Z. Kayani reported [11], and the peak at the diffraction angle equal to 26.7° which corresponds to MoO_3 [12]. The graphitic peak at about $2\theta = 28.3$ is a sharp peak [13]. The inset figure in **Fig. 3** shows XRD pattern prepared by dehydration of Iraqi date syrup, the XRD pattern for prepared graphene shows wide peak centered at $2\theta = 23.758^\circ$ at plane (002) with d-spacing $d_{002} = 3.742 \text{ \AA}$ (0.374 nm) [9].

FTIR spectroscopy helps to identify chemical bonds in molecules and this lead to the understanding of materials, the produced spectra is a sample profile which has a distinguishing fingerprint. FTIR is an active analytical tool for detecting functional groups and describing covalent bonding information. **Fig. 4** shows FTIR spectra graphene; as seen, graphene has a residual of organic functional groups and this agrees with Xiu-Zhi Tang's observation [14]. As is known that graphene was treated with a strong acid mixture to functionalize its surface and this is clear in FTIR spectra in **Fig. 5** in which graphene has many functional groups; wide peak due to intercalated water molecules ($\approx 3269.24 \text{ cm}^{-1}$) and bonded water molecules ($\approx 1733.31 \text{ cm}^{-1}$), as well as peaks for COOH (1520.77 cm^{-1}), OH (1115.25 cm^{-1}) and epoxide (1040.93 cm^{-1}), while it has stretching vibrations of Mo-O bonds at about 650 cm^{-1} as Z. Kayani [11] and Zeinab H. report [13], while the vibration at about 600 cm^{-1} refers to CoO_2 and this is associated with [11-13].

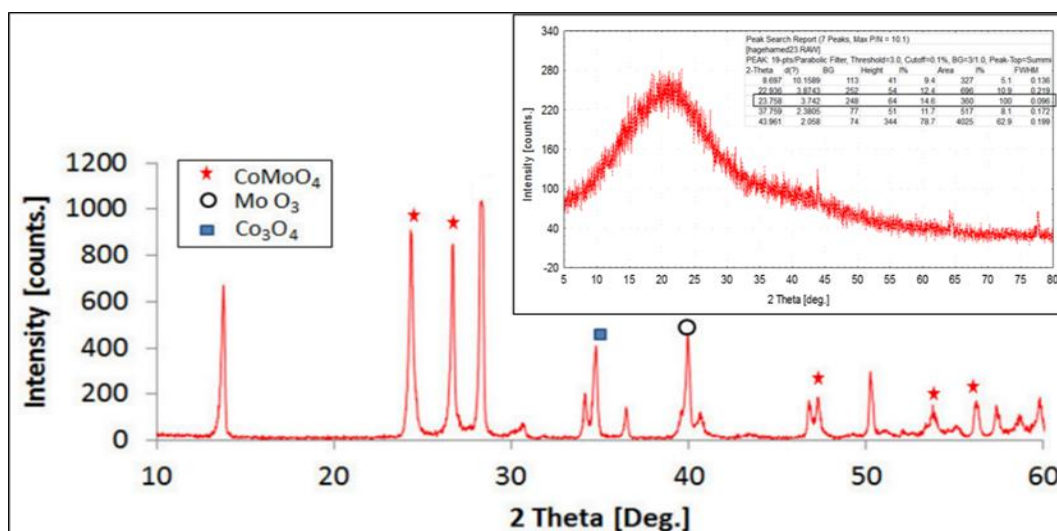


Fig. 3. XRD pattern for prepared CoMo/G catalyst which shows presence of CoMoO₄, MoO₃ and Co₃O₄ phases, while the inset figure shows XRD pattern for graphene.

Elements mapping for CoMo/G is shown in **Fig. 6**; EDS analysis shows elements mappings identify the presence of cobalt and molybdenum as well as carbon and oxygen and this analysis confirms existence of carbon 71.24 wt. %, cobalt 5.43 wt. %, and molybdenum 14.69 wt. %. The presence of molybdenum and cobalt is near the required amount (6% and 15 % for cobalt and molybdenum respectively) and this may be because of some degree of agglomeration happening during preparation as seen in SEM image in **Fig. 7**, also it can be noted that the porous structure is providing a penetration path as well for molecules or particles transferring [15]. Nano sized metal oxide particles were dispersed on Graphene sheets with a degree of agglomerate tendency from oxides molecules. The oxide particles (active and promoter phases) were dispersed on the Graphene surface with the

average particle size of about 120 nm and roughness of about 18.3 nm as seen in AFM image in **Fig. 8**. According to the BET test the graphene has the surface and pore volume of 177.96 m²/g and 0.456 m³/g respectively while the prepared catalyst has a surface area equal to 100.88 m²/g and pore volume equal 0.321 cm³/g, the surface area decrease in the case of loading molybdenum on graphene surface; Mo content will result in a low surface area due to molybdenum oxides being much denser than carbon support, for that the lowering in surface area and pore volume of CoMo/Graphene catalysts is due to high loading of molybdenum oxides and this is in agreement with Kim [16], additionally the metal oxides loading lead to blocking the pores at the Graphene surface and between Graphene layers as Speight reported [17].

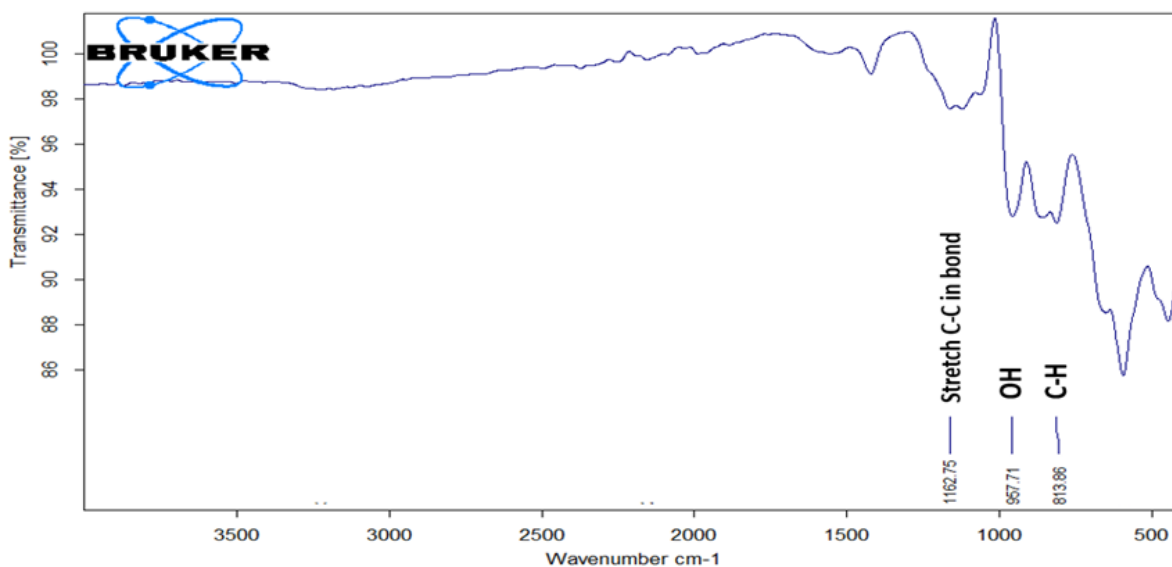


Fig. 4. FTIR spectrum for graphene.

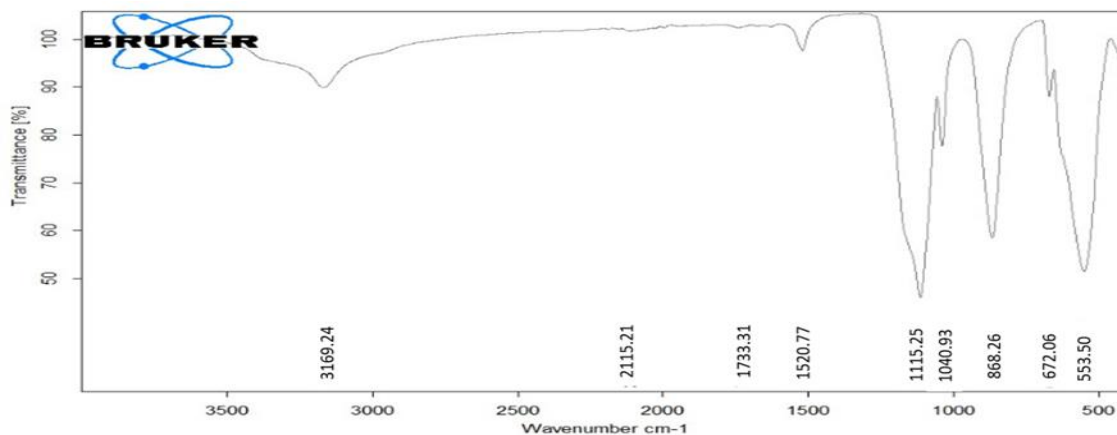


Fig. 5. FTIR spectrum for CoMo/G catalyst

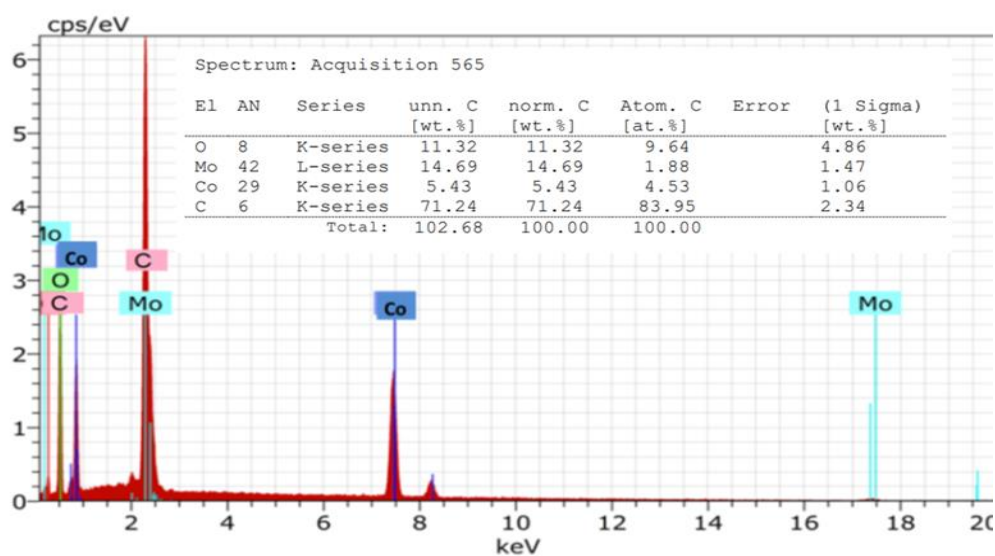


Fig. 6. EDS spectrum for CoMo/G catalyst shows the element distribution as an indication for presence of carbon, molybdenum, oxygen and cobalt with 71.24, 11.32, 11.32 and 5.43 respectively.

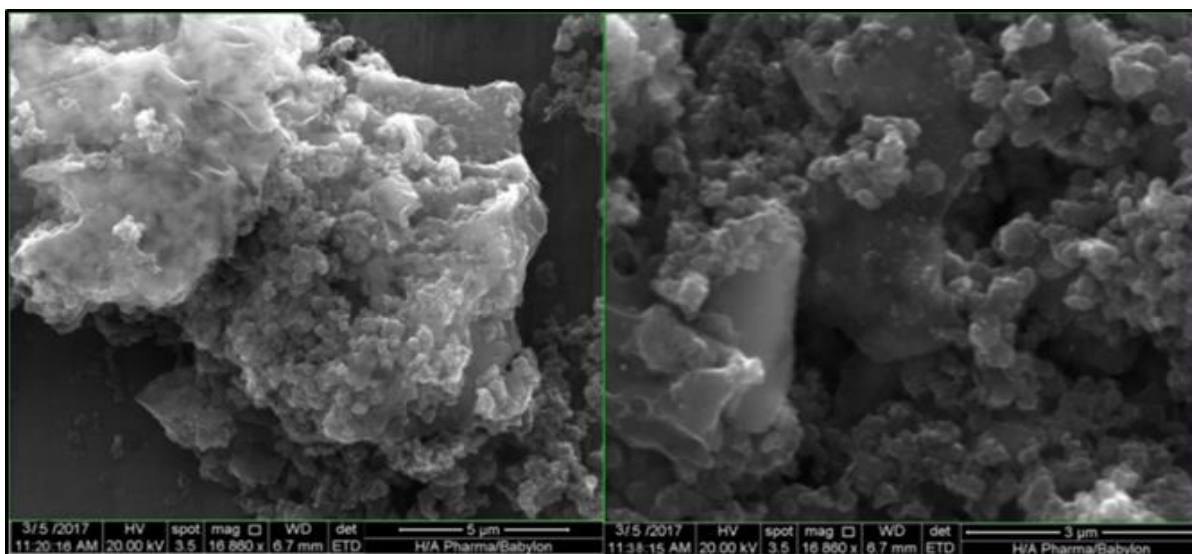


Fig. 7. SEM image for CoMo/G catalyst.

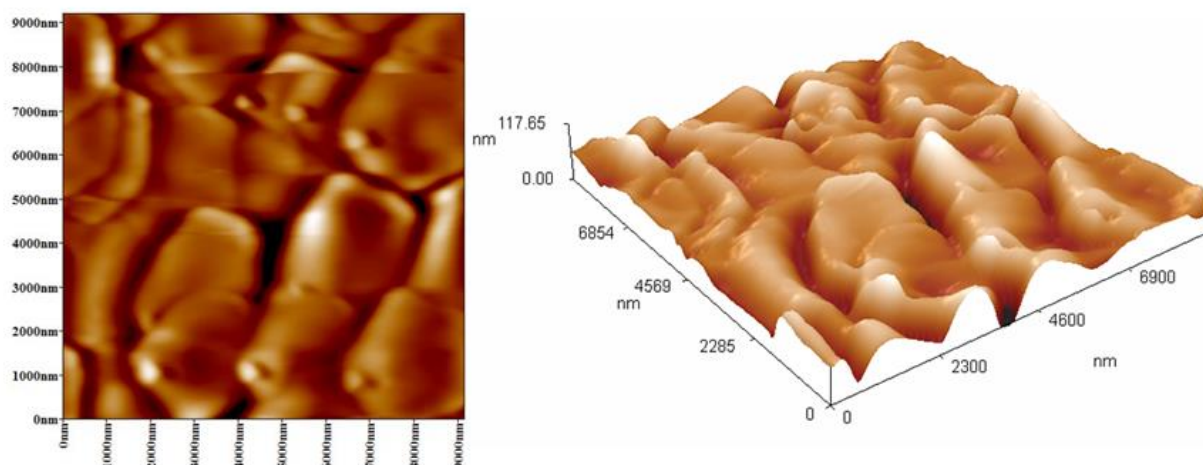


Fig. 8. 2D and 3D AFM Image for CoMo/G catalyst

3.2. Design of experiment

The experimental design method has a good ability to predict the interaction effect of studied variables as well as have many other advantages; it reduces the number of runs required to cover the effect of studied variables as well as all levels for studied variables, this method is able to predict the mathematical relationship between response and variables (studied) that can be controlled while improving the studied system. Experiment design included many methods such as Box-Wilson, Box-Behnken, Taguch, Factorial design, etc. [18]. The Taguchi method is one of the most important methods of the design of the experimental method; it was first used to improve product quality. It is similar to another experimental method by reducing the number of runs that are sufficient to cover all levels of studied variables [19].

Naphtha HDS reaction was studied under the effect of three variables (reaction temperature, LHSV and hydrogen partial pressure) and four levels for each

variable were chosen, **Table 1** shows the Taguchi method application for the present system (variables and their levels). The purpose of having HDS reaction is to increase the sulfur removing percentage product so the signal-to-noise (S/N) used in our analysis is larger is better.

The experiments results were analyzed by use of MINITAB software, in which these results were applied to the polynomial equation which related response (dependent) as a function of studied variables (independent), in most response surface methodology RSM [19], The data were then applied to the following second order polynomial equation as shown in **equation (2)**:

$$SR\% = a_0 + a_1 X_1^2 + a_2 X_2^2 + a_3 X_3^2 + a_4 X_1 + a_5 X_2 + a_6 X_3 + a_7 X_1 X_2 + a_8 X_1 X_3 + a_9 X_2 X_3 \quad (2)$$

Table 1. List of independent (controllable) variables and their levels.

Controllable variables	level			
	1	2	3	4
Reaction temperature (°K)	523	548	573	598
LHSV (hr. ⁻¹)	3	4	5	6
Hydrogen pressure (bar)	10	11	12	13

Where, $SR\%$ is sulfur content in final product, X_1 represents reaction temperature, X_2 represents liquid Hourly Space velocity, X_3 represents pressure, and $a_0, a_1, a_2 \dots a_9$ are the second order parameters.

According to Taguchi experimental design, study needs to identify objective of design, or specify signal-to-noise S/N ratio; Taguchi method proposed many expressions to S/N calculation. The purpose of this work is to increase sulfur removal $SR\%$ in the final product, thus S/N ratio was applied here as following (equation 3):

$$larger\ is\ better : SN_s = -10 \log \left(\frac{\sum_{i=1}^n (1/y_i^2)}{n} \right) \quad (3)$$

Where, n = sample size, and y = surface roughness in that run [17] (Table 2). Fig. 9 shows parameters levels corresponding to S/N ratio was calculated according to equation (3) for the general trend for effect of variables on $SR\%$. According to Taguchi method, the analysis shows sulfur removal $SR\%$ of final product increased with increasing the reaction temperature and pressure, while it increased with increasing space velocity LHSV and this is in agreement with literatures [20-22]. The results obtained by this Taguchi method were formed as an equation by MINITAB software, equation (4):

$$SR\% = 31.46 - 0.375 X_1^2 - 0.625 X_2^2 - 0.75 X_3^2 + 9.238 X_1 - 5.236 X_2 + 11.977 X_3 + 1.045 X_1 X_2 - 0.867 X_1 X_3 + 0.909 X_2 X_3 \quad (4)$$

3.3. Effect of controlled variables on sulfur removal

The studying of impact studied (controlled) variables done by application equation (4) which can be acceptable because high correlation factor R^2 (0.98) means that the error between actual and theoretical values was negligible.

3.3.1. Temperature effect on sulfur removal

An increase in temperature leads to an increase in desulfurization, as can be seen in Fig. 10, it is clear that increasing the temperature causes an increase in the internal motion of molecules, which results in an increase in producible collisions between molecules and thus directing the reaction to the forward direction of the desulfurization reaction between hydrogen and sulfur organic compounds, as reported in many previous literatures [20-22].

Table 2. Taguchi’s Orthogonal Array L^{16} , with 3 variables and 4 levels each and measured results according to Taguchi method experimental design.

Run	Code value			Rael value			Sulfur content	SR%
	A	B	C	T(°K)	LHSV (hr ⁻¹)	P(bar)	ppm	
1	1	1	1	523	3	10	395	48
2	1	2	2	523	4	11	362	52
3	1	3	3	523	5	12	316	58
4	1	4	4	523	6	13	298	61
5	2	1	2	548	3	11	283	63
6	2	2	1	548	4	10	368	51
7	2	3	4	548	5	13	202	73
8	2	4	3	548	6	12	297	61
9	3	1	3	573	3	12	159	79
10	3	2	4	573	4	13	127	83
11	3	3	1	573	5	10	331	56
12	3	4	2	573	6	11	292	61
13	4	1	4	598	3	13	105	86
14	4	2	3	598	4	12	127	83
15	4	3	2	598	5	11	203	73
16	4	4	1	598	6	1	305	60

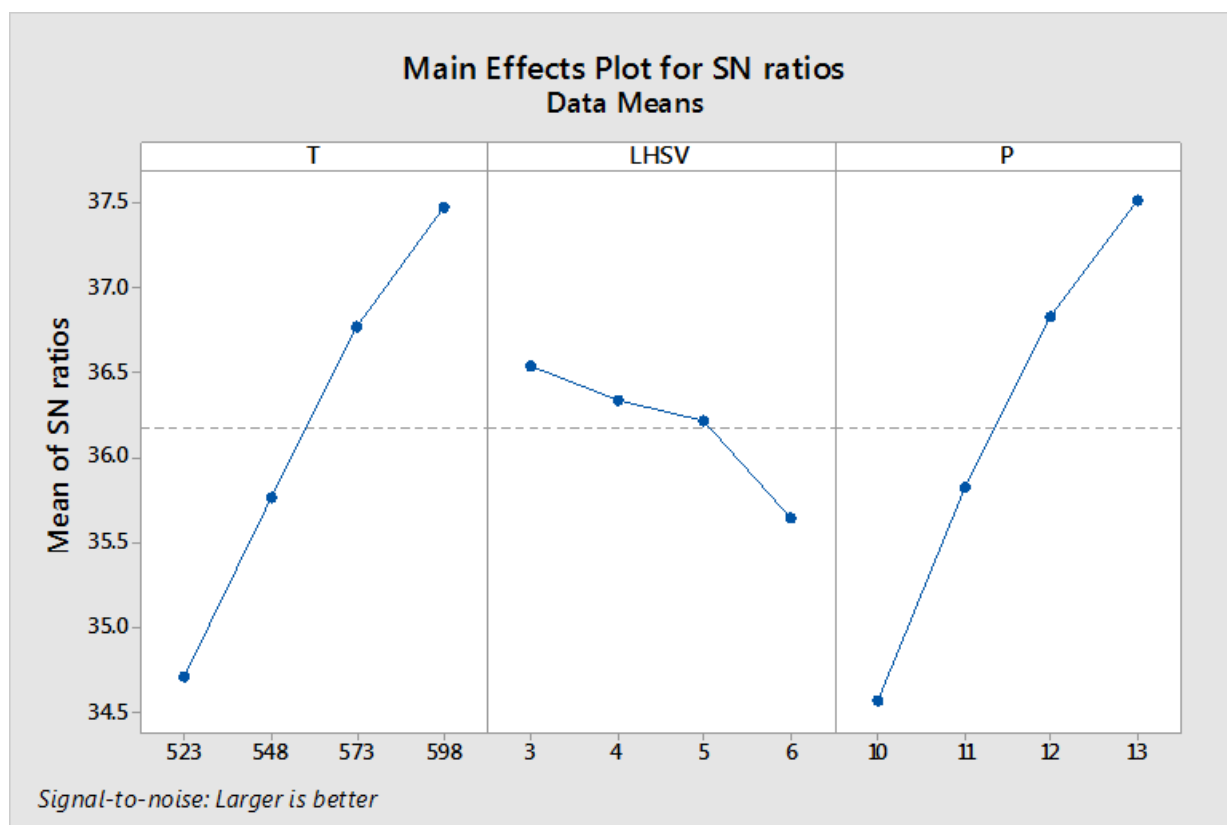


Fig. 9. The parameter levels corresponding to larger S/N ratio were chosen to optimizing conditions. The general trend effect for reaction temperature, LHSV, and pressure on SR% for HDS reaction at CoMo/G catalyst, the optimum condition to get maximum sulfur removal efficiency with increasing reaction temperature and hydrogen pressure and with decreasing space velocity LHSV.

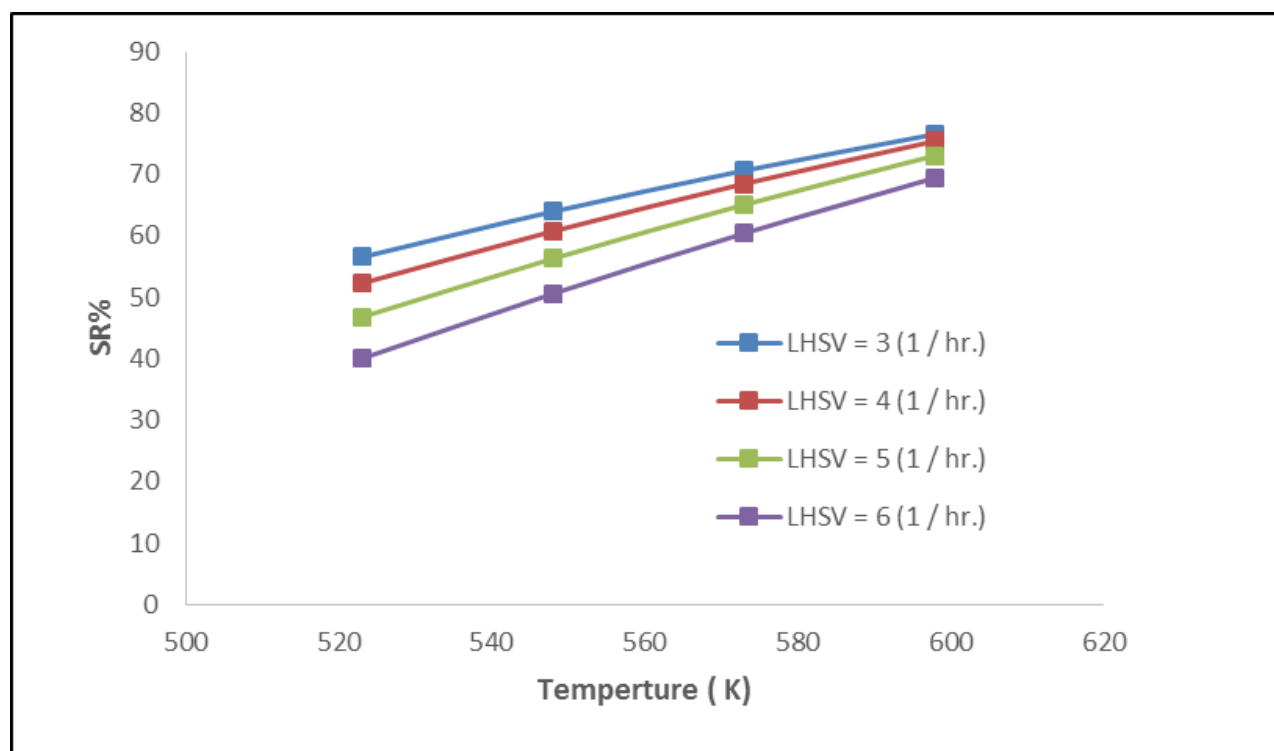


Fig. 10. Effect of temperature at different LHSVs on removal of sulfur from naphtha by using CoMo/G catalyst at constant pressure 1.1 MPa and Gas/oil ratio 50 ml/ml, the sulfur removal efficiency increasing with reaction temperature at the same value of space velocity LHSV.

3.3.2. Space velocity effect on sulfur removal

Fig. 11 shows the effect of increasing space velocity on hydro-desulfurization reaction, the LHSV increasing caused decrease in sulfur removal percentage i.e. at temperature 598 K the sulfur removal reduced from 75% at LHSV 3 hr.⁻¹ to 66% at LHSV 6 hr.⁻¹, the increase in space velocity cause a decrease in contact time between reactants so the probability of reaction happening was minimized [23, 24].

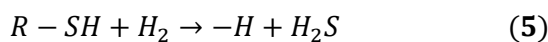
3.3.3. Effect of hydrogen pressure

An increase in the pressure of hydrogen leads to an increase in the conversion of the reaction or increasing sulfur removal, the increase in pressure leads to a decrease in the formation of coke on the surface of the catalyst, which means the chance of the reaction occurring grows with increasing pressure [5]. The increase in sulfur removal due to increased pressure leads to the hydrolysis of the organic sulfur compounds, as reported by H.T (Fig. 12). Sayed [25]. Changlong Yin suggests that the HDS product was very sensitive to the pressure of the reaction, especially at low pressure near 1 MPa, which caused naphtha cracking on the catalyst surface, thus increasing the pressure will enhance the HDS product [20].

3.4. HDS reaction kinetics

There are many methods used to estimate kinetics parameters (rate constant, reaction order and activation energy), for example power law, integral analysis and differential analysis, but here we will be using power law and a statistical technique called Levenberg-Marquardt algorithm, used to solve nonlinear problems by fitting reported data with a suggest model; this technique is a combination of two minimization methods; Gauss-Newton method and gradient descent method, and the model was calculated by of SPSS software version 20.

By assuming the HDS reaction is from nth order, and that the R-SH is represented as the sulfur compounds presence within fuel, so the chemical equation is written as follow (equation 5):



where S refers to R-SH, thus rate equation can be written as (equation 6):

$$\frac{dS}{dt} = -kS^n P_{H_2}^a \quad (6)$$

Where (dS / dt) is the rate of disappearance sulfur with time, k is reaction rate constant, S sulfur concentration [mg / kg] at time t [hr.], n is reaction order in respect to sulfur concentration, p is hydrogen pressure [MPa], and a is hydrogen pressure index. The integration for equation (6) leads to equation (7)

$$S_f^{1-n} - S_o^{1-n} = (n - 1)kP_{H_2}^a t \quad (7)$$

In which S_f is the final sulfur concentration, and S_o is the initial sulfur concentration.

To introduce LHSV in kinetic equation, by opposite of time with power b which is introduced to use LHSV [1 / hr.] in equation (7), the equation (8) is written as follows:

$$S_f^{1-n} - S_o^{1-n} = (n - 1)kP_{H_2}^a (LHSV)^b \quad (8)$$

Reaction rate constant can be expressed by Arrhenius equation (9):

$$k = k_0 \exp\left(-\frac{E}{RT}\right) \quad (9)$$

And by inserting equation (9) into equation (8), we get equation (10):

$$S_f^{1-n} - S_o^{1-n} = (n - 1)k_0 P_{H_2}^a (LHSV)^b \quad (10)$$

Rearrange equation (10) leads to get equation (11):

$$S_f = [(n - 1)k_0 P_{H_2}^a (LHSV)^b \exp\left(-\frac{E}{RT}\right) + S_o^{1-n}]^{\frac{1}{1-n}} \quad (11)$$

Where k_0 is the pre-exponential factor of Arrhenius equation; E is the apparent activation energy of reaction [kJ/mol]; T is reaction temperature, K; and R is universal gas constant [8.314 J/ mol · K]. Equation (11) represents the sulfur concentration in the final product as a function of experimental variables (temperature, space velocity and pressure) with kinetics parameters (activation energy, reaction order and rate constant).

As mentioned above, the Levenberg-Marquardt method was chosen for estimation of the kinetic parameters (a , b , n , k_0 and E), The experimental data (see Table 2) were calculated with the software SPSS 20 (SPSS, Inc., Chicago, IL, USA) and were incorporated into the Levenberg–Marquardt method. The parameters of the kinetic equation were found as:

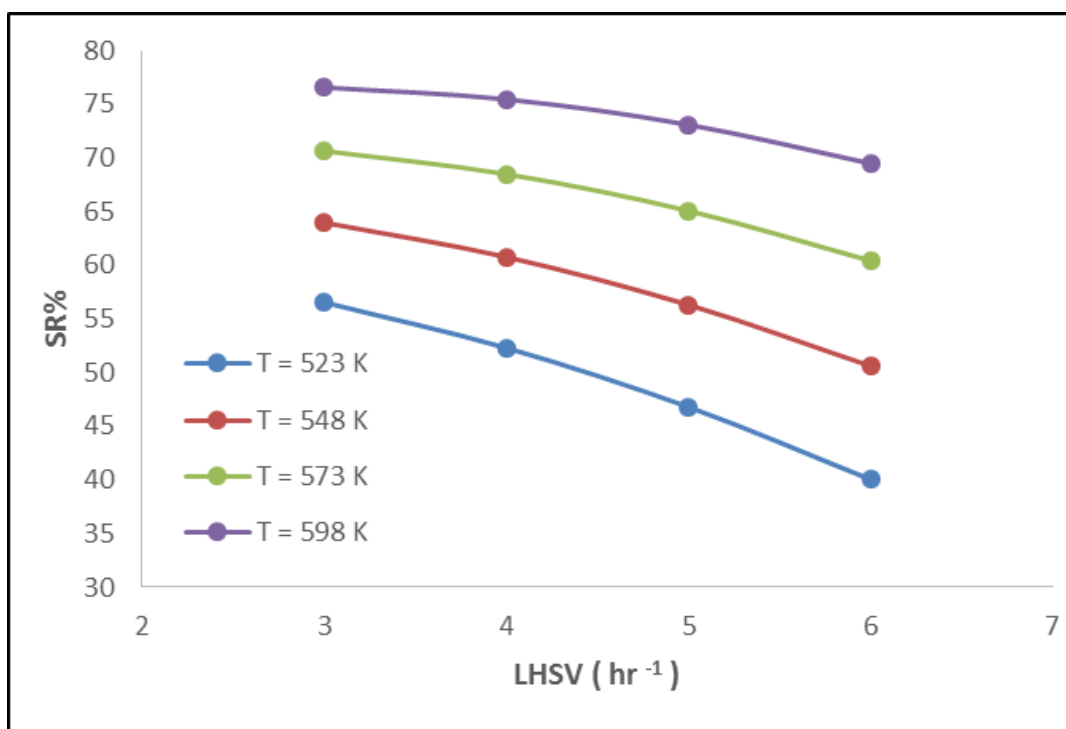


Fig. 11. Effect of LHSV at different temperatures on removal of sulfur from naphtha by using CoMo/G catalyst at constant pressure=1.1 MPa and Gas/oil ratio 50 ml/ml, the sulfur removal efficiency decreasing with space velocity LHSV at same reaction temperature.

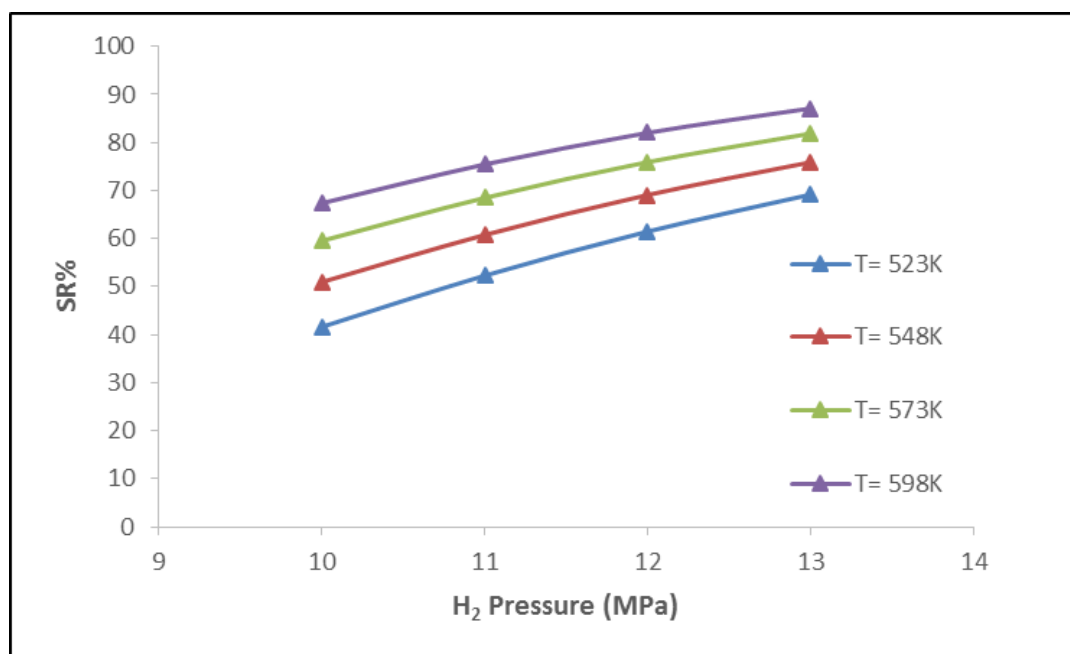


Fig. 12. Pressure effect on removal of sulfur from naphtha by using CoMo/G catalyst at constant LHSV=4 hr.⁻¹ and Gas/oil ratio 50 ml/ml, the sulfur removal efficiency increasing with hydrogen pressure at the constant reaction temperature.

$E = 32.309$, $a = 3.716$, $b = -0.576$, $n = 1.863$, $k_0 = 4.753$
and $R^2 = 0.996$.

And **equation (11)** can be written in term of kinetics parameters predicted by Levenberg-Marquardt non-linear regression as follows (**equation 12**):

$$S_f = \left[4.10 P_{H_2}^{3.716} (LHSV)^{-0.576} \exp\left(-\frac{32309}{RT}\right) + S_0^{-0.863} \right]^{-1.159} \quad (12)$$

4. Conclusions

The sulfur removal efficiency ranged from 32% at (temperature = 523 K, LHSV = 3 hr.⁻¹ and hydrogen pressure = 10 bar) to 79% at (temperature = 598 K, LHSV = 3 hr.⁻¹ and hydrogen pressure = 13 bar) According to Taguchi method analysis, the heavy naphtha HDS reaction shows that the effects of variables on reaction activity follow a general trend in which sulfur removal increases with temperature and pressure increasing and decreases with the increase of space velocity. The system for HDS process was described by second order polynomial and indicates high accuracy for predicted sulfur content in the final product as a function of studied variables (temperature, pressure and LHSV). Levenberg- Marquardt algorithm helps to estimate kinetics parameters by curve fitting for reported results with kinetic model driven proposed from rate equation for nth order reaction, which gives high R²=0.996 and the kinetics parameters are: E = 32.309 KJ/mol., and n = 1.863.

References

- [1]. Chen, T.-M., WG Kuschner, J Gokhale and, S Shofer., *Amer. J. Med. Sci.*, 333(4) , (2007), 249-256.
- [2]. S Liu, B Wang, BCui and, L Sun, *Fuel*, 87(3), (2008), 422-428.
- [3]. I. Mohammed, H. H. Alwan, Ghanim A. N, IOP Conference Series: Mater. Sci. Eng. 928, (2020), 022158.
- [4]. S Cristol, J F Paul, E Payen, D Bougeard, F Hutschka and, S Clemendot, *J. Catal.* 224 (1) (2004), 138-147.
- [5]. A Kundu, K.D.P. Nigam, A.M. Duquenne and, H. Delmas, *Rev. Chem. Eng.*, 19 (6), (2003), 531-605.
- [6]. Z. Hajjar, M. Kazemeini, A. Rashidi, M. Bazmi, *Catal. Let.*, 145 (9) (2015), 1660-1672.
- [7]. H. H. Alwan, Ammar A. Ali, and Hassan F. Makki, *Bullet. Chem. React. Eng. Catal.* 15 (1) (2020), 175-185.
- [8]. Jéssica Rabelo do Nascimento, Monique Ribeiro D'Oliveira, Amanda Garcez Veiga, Carlos Alberto Chagas, and Martin Schma, *ACS Omega* , 5 (40) (2020), 25568-25581.
- [9]. Hasan F. Makki and H. H. Alwan, *AAUJES*, 26 (1) (2019), 49-54.
- [10]. Shyamal. K. Bej, R. P. Dabral, P. C. Gupta, K. K. Mittal, G. S. Sen, V. K. Kapoor, and Ajay K. Dalai, *Energ. Fuels*, 14 (3) (2000), 701-705.
- [11]. Z. N. Kayani, S. Arshad, S. Riza, R. Zia and, S. Naseem, *JOAM*, 11 (12) (2009), 2141-2144.
- [12]. Jong-Pil Jegal, Hyun-Kyung Kim, Jeom- S0 Kim and, Kwang -Bum Kim, *J. Electroceram.*, 31 (1-2) (2013), 218-223.
- [13]. Z. Hajjar, M. Kazemeini, A. Rashidi, M. Bazmi, *Fuel*, 165 (2016), 468-476.
- [14]. T. Wei, Z. Fan, G. Luo, C. Zhang and, D. Xie, *Carbon*, 47 (1) (2009), 337-339.
- [15]. A. T. Bell, *Science*, 299 (5613) (2003), 1688-1691.
- [16]. S. Ki Kim, D. Yoon, S. Cheol Lee and, J. Kim, *ACS Catal.*, 5 (6), (2015), 3292-3303.
- [17]. James G. Speight, *The desulfurization of heavy oils and residua*. 1999, second edition, CRC Press.
- [18]. S. Athreya and Dr Y.D.Venkatesh, *IRJES* ,1 (3) (2012), 13-19.
- [19]. Z. R. Lazic, *Design of experiments in chemical engineering: a practical guide*. (2004), John Wiley & Sons.
- [20]. C. Yin, R Zhao and Chenguang, *Energ. Fuels* , 17 (5) (2003), 1356-1359.
- [21]. X. Lan, C. Xu, G. Wang and, J. Gao, *Catal. Today* 140 (3-4), (2009), 174-178.
- [22]. J.V.Lauritsen , M. Nyberg , J.K. Norsjov , B.S. Clausen , H Topsoe , E. Laegssgaard and , F. Bensenbacher , *J. Catal.* 224 (1) (2004) 94-106.
- [23]. J. Ancheyta , M.J. Angeles , M. J. Maciad , G. Marroquin and, R. Morales , *Energ. Fuels* 16 (1) , (2002), 189-193.
- [24]. Gopal H. Singhal, Ramon L. Espino, Jay E. Sobal and G.A. Huff, *J. Catal.* 67 (2) , (1981), 457-468.
- [25]. Syed Tajammul Hussein, F. Zia and M. Mazjar, *Eur. Food Res. Tech.*, 228 (5) (2009), 799-806.